

Effects of La Exchange on NaY and NaX Zeolites As Characterized by ^{29}Si NMR

Kristin Gaare

Department of Chemistry, University of Oslo, P.O. Box 1033 Blindern, N-0315 Oslo, Norway

Duncan Akporiaye*

SINTEF Applied Chemistry, P.O. Box 124 Blindern, N-0314 Oslo, Norway

Received: July 8, 1996; In Final Form: September 15, 1996[®]

The effects of lanthanum exchange in zeolite Y and zeolite X were studied by ^{29}Si NMR. The spectra of calcined LaNaY were curve-fitted by two functions derived from the spectrum of pure NaY, by keeping the Si/Al ratios of the two functions constant and similar to NaY. The fraction of the spectra shifted upfield as a result of lanthanum migration was consistent with the percent La exchange and not with the fractional occupancy of the Si' sites. Curve fitting of ^{29}Si NMR spectra of LaNaX was more complicated due to a selective ion exchange of cations close to the $\text{Si}(4\text{Al})$ sites in zeolite X. However, when a redistribution of intensity between the two functions was allowed, while keeping the overall Si/Al ratio constant, high consistency between the observed and simulated spectra of LaNaX was found. It is evident from this work that the influence of lanthanum is different for the two zeolites. The results from the combination of the selective ion exchange and ^{29}Si NMR spectra of LaNaX were found to correlate with those from Monte Carlo simulations and may be used as a complement in the study of the local ordering of framework elements.

Introduction

The modification of zeolites by ion exchange of exchangeable cations provides a useful means of tailoring their properties to particular applications. Thus, the introduction of rare-earth elements, in particular into zeolite Y, has been an important means of enhancing the performance of, for example, FCC catalysts,¹ and they are also known to increase the activity of the zeolite in a variety of reactions due to the increased acid strength.²

In addition to the important modification of the catalytic properties of the zeolite, the detailed changes in the state and location of lanthanum during thermal treatment have also attracted interest. As has been documented by a variety of studies,³ the initial hydrated cation $\text{La}(\text{H}_2\text{O})^{3+}$ in the hydrated zeolite before thermal treatment is located within the large supercage of zeolite Y at the SII and SV sites; see Figure 1. Subsequent thermal treatment at temperatures as low as 80 °C initiates a process of dehydration/dehydroxylation of the cation, which allows it to migrate through the six-ring opening of the sodalite cage and reside in the SI or Si' sites.⁴ Early structural studies⁵ and recent modeling calculations⁶ point to the Si' site as the favored site for the dehydrated cation, despite the greater opportunity for 6-fold coordination within the double six-ring.

Multinuclear solid state NMR spectroscopy is one technique that has given valuable insight into the migration of the La and Na cations during thermal treatment. ^{139}La NMR has been used to differentiate between the highly mobile hydrated lanthanum cation in the supercage and the more restricted location of the dehydrated cation within the sodalite cage.^{7–9} Conversely, ^{23}Na NMR has been used to monitor the location of the sodium cations in a variety of exchange sites and, through careful study, can be used to observe which sites are preferentially depleted during the introduction and migration of the lanthanum cation.^{8,10}

^{29}Si NMR, in a more indirect study of the zeolite framework, has also been shown to be sensitive to the presence of lanthanum

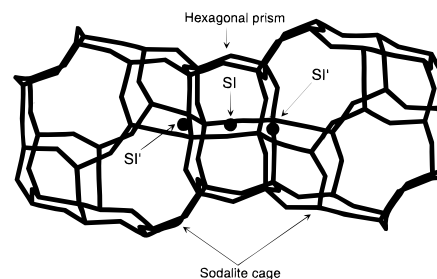


Figure 1. Sodalite cage and hexagonal prism in the framework of faujasite. The circles indicate the cation positions; the SI site is at the center of a hexagonal prism, and the Si' is in the sodalite cage close to the center of a six-ring belonging to a hexagonal prism.

within the sodalite cage after thermal treatment. In particular, it is evident that when lanthanum is located in the sodalite cage, the silicon atoms within the local sphere of influence undergo a ca. 3 ppm high-field shift with respect to the normal peak position. Thus, two nearly overlapping sets of spectra could be distinguished, and the relative ratios of the areas were proposed as giving a direct representation of the La/Na composition.¹¹

Of all the reported NMR studies of the location and migration of La in the faujasite structure, the primary focus has been the Y form of the faujasite structure. Despite the industrial importance of this form, studies on this system have an inherent limitation in the range of compositions that can be accessed, since the lowest achievable Si/Al ratio for this form is ca. 2.5. At this limiting composition, the maximum number of La cations that can be exchanged into the zeolite (assuming a +3 charge on lanthanum), is ca. 18 per unit cell, this being equivalent to only a 56% occupancy of the 32 available Si' sites, the preferred location within the sodalite cage. In contrast, the X form of faujasite, which has a limiting framework composition of Si/Al = 1, offers the opportunity of achieving a greater than 80% filling of the Si' sites.

In our studies of the catalytic properties of lanthanum-exchanged faujasite zeolites in Friedel–Crafts acylation reac-

* To whom correspondence should be addressed. FAX +47 22 06 73 50, e-mail duncan.akporiaye@si.sintef.no.

[®] Abstract published in *Advance ACS Abstracts*, December 1, 1996.

tions,¹² we have prepared LaX and LaY zeolites at a variety of exchange levels and have carried out detailed characterization using ²⁹Si NMR and high-resolution diffraction. This has given us the opportunity to carry out the first reported complementary study of LaY and LaX in this way. In this work, we have also addressed one evident inconsistency in the reported study of Chao et al.¹¹ As supported by all reported work on the LaY system, their working hypothesis for the assignments of the spectra are as follows: (a) hydrated (never calcined) LaY = hydrated La³⁺ on SII site in supercage = no perturbation of the ²⁹Si spectra; (b) calcined LaY = dehydrated La³⁺ on SI' site in sodalite cage = strong perturbation of the ²⁹Si spectra.

At a maximum lanthanum loading of the SI' sites of 56%, it is evidently not possible for all the silicons in the framework to be directly influenced by a lanthanum cation. Thus, it could be expected that the fraction of the NMR spectrum affected by the lanthanum exchange would be proportional to the *fractional occupancy of the SI' sites*. However, the observed results indicate that this is not the case and that the affected part of the spectrum is proportional to the *total fraction of sodium replaced by lanthanum*.

Experimental Section

Materials. The zeolites studied in the present work are commercial products of zeolite X and zeolite Y. The zeolite X with the unit cell composition Na_{83.5}Al_{83.5}Si_{108.5}O₃₈₄·H₂O (Union Carbide type 13X, Si/Al = 1.3) was provided by Fluka, and the zeolite Y (LZ-Y52, Si/Al = 2.5) with the unit cell composition Na_{54.9}Al_{54.9}Si_{137.1}O₃₈₄·H₂O was provided by Aldrich.

Samples with different levels of La exchange were obtained from NaX and NaY by ion exchange with different amounts of La(NO₃)₃, according to a literature procedure.¹³ The ion-exchange procedure used for NaX and NaY was as follows: 40 g of the zeolite was suspended in 3 L of deionized water. A calculated amount of La(NO₃)₃·6H₂O was dissolved in 100 mL of deionized water and was added dropwise to the zeolite at ambient temperature during 1 h. The suspension was then stirred at 70 °C for 24 h before the slurry was filtered and the material washed with deionized water. The following work-up for zeolite Y and zeolite X will be described separately.

LaNaY. The products were finally dried in air at 100 °C for 24 h. Samples with different levels of lanthanum exchange were obtained; the percentage of the theoretically possible ion-exchange capacity (*N_{Al}* divided by 3 to compensate for the charge difference between Na⁺ and La³⁺) is given in parentheses for the sample notation. Samples with 41% La(41)NaY and 74% La(74)NaY lanthanum exchange were obtained from NaY, as confirmed by elemental analysis.

La(100)Y was made from La(74)NaY by a second ion exchange: 8.6 g of La(74)NaY was calcined at 400 °C for 7 h in flowing air before it was suspended in 650 mL of deionized water. A 2.4 g sample of La(NO₃)₃·6H₂O dissolved in 10 mL of deionized water was added dropwise at ambient temperature, and the suspension was then stirred at 70 °C for 24 h. Finally, the zeolite was filtered, washed with deionized water, and dried at 100 °C.

LaNaX. The following exchange levels were obtained from NaX by ion exchange with La(NO₃)₃ at 70 °C: La(20)NaX, La(42)NaX, La(59)NaX, and La(79)NaX. After the ion exchange and subsequent washing, the filtrated zeolites La(20)-NaX, La(59)NaX, and La(79)NaX were finally air dried at ambient temperature, while La(42)NaX was dried at 100 °C for 24 h.

La(97)NaX was made from NaX by ion exchange with La(NO₃)₃ at 70 °C by the same procedure as described above,

TABLE 1: Number of Lanthanum Cations per Unit Cell in LaNaY and LaNaX Zeolites

zeolite	La ³⁺ /uc	zeolite	La ³⁺ /uc
La(41)NaY	7.7	La(42)NaX	12.3
La(74)NaY	13.5	La(59)NaX	17.8
La(100)Y	18.8	La(79)NaX	23.8
La(20)NaX	5.9	La(97)NaX	29

followed by calcination and a second ion exchange: After the first ion exchange the zeolite was filtered and washed with deionized water. This partly exchanged LaNaX was dried at 100 °C over night before it was calcined (1 h at 200 °C, 1 h at 300 °C, and 7 h at 400 °C) in flowing air. After the calcination the zeolite was stored 1 night in a desiccator with a water-saturated atmosphere before it was subjected to a second ion exchange with La(NO₃)₃ at 70 °C for 24 h. After filtration and washing, the resultant material was dried at 100 °C for 3 days. The lanthanum-exchanged zeolites are summarized in Table 1.

NMR Spectroscopy. **LaNaY.** The LaNaY zeolites were calcined at 450 °C under a vacuum of 0.01 mbar overnight before they were introduced into the MAS rotor under dry argon in a glovebox. A sample of La(41)NaY was stored over saturated NH₄Cl solution at ambient temperature to obtain a fully hydrated zeolite prior to the NMR analysis. The MAS NMR spectra were recorded on a Varian VXR 300 S WB NMR spectrometer equipped with 7 mm zirconia rotors. Conditions for the ²⁹Si MAS NMR spectra were as follows: resonance frequency, 59.6 MHz; sweep width, 14 000 Hz; pw(90), repetition time 10 s. All chemical shifts are referenced to tetramethylsilane used as external standard.

LaNaX. NMR was performed on as-exchanged and calcined samples of LaNaX. The LaNaX zeolites were calcined for 7 h in flowing air. They were stored in a sealed sample holder a few days before they were introduced into the MAS rotor. A glovebox was not used when these samples were filled into the rotor; these samples may therefore be regarded as partially rehydrated. The MAS NMR spectra of as-exchanged and calcined samples of La(20)NaX, La(59)NaX, and La(79)NaX were recorded on a Bruker 200 Avance DMX spectrometer equipped with a 4 mm zirconia rotor under the following conditions: resonance frequency, 39.7 MHz; sweep width, 19 800 Hz; pw(90), repetition time 10 s. The MAS NMR spectra of NaX (as-synthesized) La(42)NaX (calcined), and La(97)NaX (calcined) were recorded on the same 300 MHz instrument as the Y zeolites.

The MAS NMR spectra were curve-fitted using the PC programs Excel and Microcal Origin.

Characterization. Chemical analysis was performed on a Siemens SRS 303 AS X-ray wavelength dispersive fluorescence spectrometer where the samples were analyzed as fused beads. The relative uncertainty for each element is 1%.

In order to check the crystallinity of the zeolites, X-ray powder diffraction was performed on a Siemens D5000 diffractometer, using nickel-filtered Cu Kα radiation.

TGA of La(74)NaY was performed on a Perkin-Elmer TGA 7. Most of the weight loss is observed below 150 °C and is due to adsorbed water. If 255 water molecules per unit cell is assumed,⁴ approximately 20 water molecules remain in the zeolite after calcination at 450 °C.

Results

Zeolite Y. In Figure 2 the ²⁹Si spectra of the different LaNaY zeolites are presented. The distinct signals correspond to Si(*n*Al) tetrahedra of the zeolite framework in different chemical environments. As the number *n* of Al atoms increases, the peaks are systematically shifted about 4 ppm to lower magnetic field, from −103.4 ppm for Si(0Al) to −90.5 for the Si(3Al) in NaY.

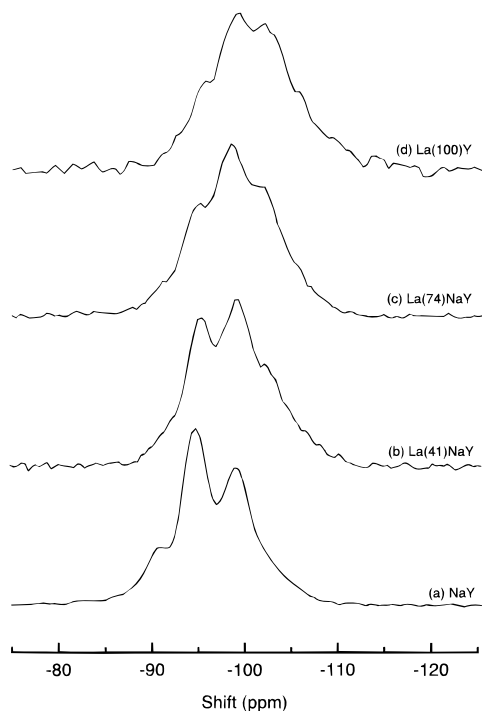


Figure 2. ^{29}Si MAS NMR spectra of calcined samples of LaNaY and NaY: (a) NaY, (b) La(41)NaY, (c) La(74)NaY, and (d) La(100)Y.

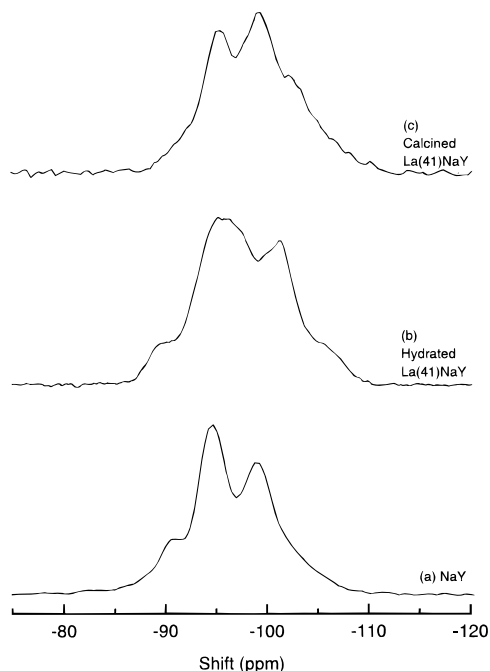


Figure 3. ^{29}Si MAS NMR spectra of La(41)NaY and NaY: (a) NaY, (b) hydrated La(41)NaY, and (c) calcined La(41)NaY.

The figure clearly shows a gradual change in the spectra with the level of lanthanum, with a high-field shift of about 3 ppm for the La-exchanged zeolites with respect to NaY.

The ^{29}Si spectra of La(41)NaY, hydrated and calcined at 450 °C, are compared with NaY in Figure 3. The chemical shift and line shape of the hydrated sample are very similar to those of NaY, while the spectrum of the calcined sample has a different shape and chemical shift. Chao et al. made the same observation in a study of the effect of hydration and dehydration on ^{29}Si NMR spectra of Y zeolites containing various extraframework cations.¹⁴ The hydrated lanthanum cations cannot enter the sodalite cage due to the large radius, and the $[\text{SiO}_4]$ tetrahedra are not perturbed by the lanthanum cations in the supercage due to a rapid motion and shielding of the charge in

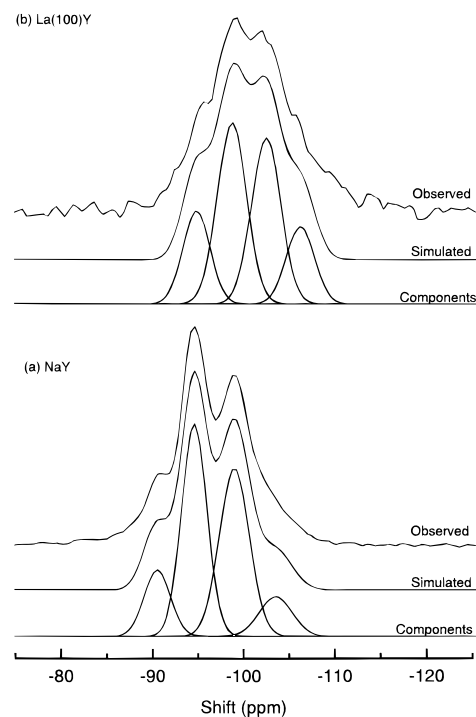


Figure 4. ^{29}Si MAS NMR spectra of (a) NaY and (b) La(100)Y (calcined) decomposed into the constituent peaks.

the hydrous environment. When the zeolite is calcined, the hydrated La^{3+} cation strips of the water molecules and migrates to positions in the sodalite cage. This process starts at 80 °C, and the creation of Brønsted acid sites as a consequence is well-documented.¹⁵ The high-field shift has been attributed to the increased strain of the Si—O—T (T = Al or Si) bonds in the six-ring window close to the lanthanum cation at position SI' in the sodalite cage.³ Thus, the spectrum of dehydrated partially ion-exchanged LaNaY consists of a superimposition of two sets of Si(*n*Al) lines, which result in a line shape different from the parent material. Figure 3 shows some differences between the spectra of NaY and hydrated La(41)NaY. The difference can be explained by the work-up procedure for the Y zeolites. As described in the Experimental Section, the LaNaY zeolites were dried at 100 °C after the ion exchange. During this drying some of the cations have already migrated to the sodalite cage.

Curve Fitting of LaNaY. The decomposition of NaY and La(100)Y spectra into the constituent peaks are presented in Figure 4. From the known relationship between the Si/Al ratio and the area of the peaks, the Si/Al ratio was found to be 2.5 for NaY and 2.6 for La(100)Y.¹⁶ The Si(4Al) peak was included to describe the spectrum of NaY when this was used in the curve fitting of LaNaY as described below, in order to obtain the least difference between the simulated and observed spectrum of NaY. The Si/Al ratio of this deconvolution was also found to be 2.5.

The curve fitting of LaNaY was performed according to the following procedure: The ^{29}Si NMR spectrum of NaY was decomposed into five peaks, each with a Gaussian line shape. These five peaks were put into one function called **NaY**. For the function **NaY**, the line width, chemical shift, and amplitude can be varied, while the relative area ratios of its constituent peaks will remain constant. As described above, the spectrum of a partly ion-exchanged LaNaY consists of two nearly overlapping spectra. The unperturbed part of the spectrum can be described by the function **NaY**, and the perturbed part of the spectrum can be described by a function **LaY**, this being similar to **NaY** except for a high-field shift of approximately 3 ppm. Accordingly, only the spectrum of pure NaY was used

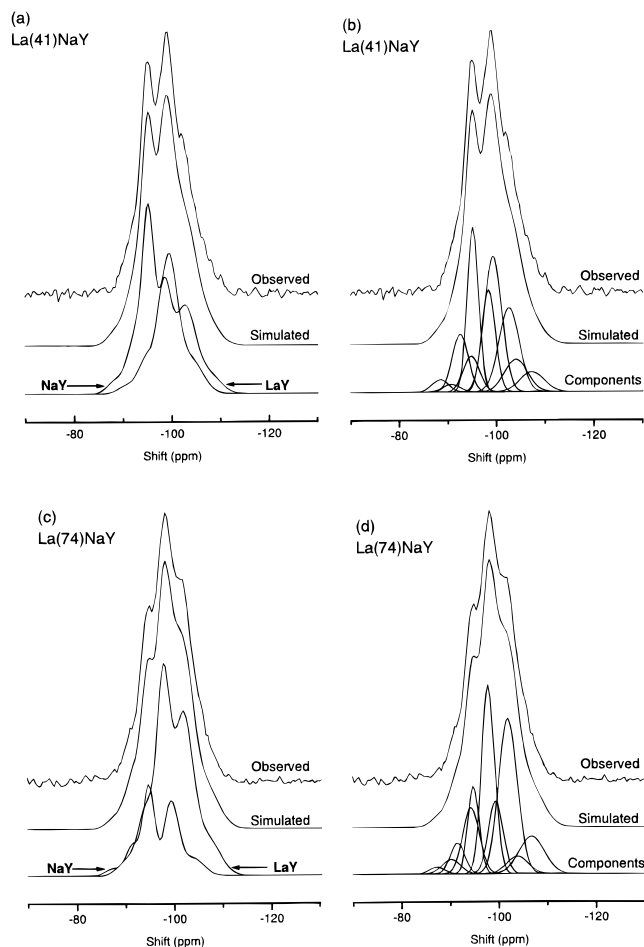


Figure 5. Observed and curve-fitted ^{29}Si MAS NMR spectra of calcined samples of La(41)NaY (a, b) and La(74)NaY (c, d), including the Na and La component profiles (a, c) and full curve fitting, with all 10 peaks visible (b, d).

TABLE 2: Percent La Exchange in LaNaY Zeolites Determined by Chemical Analysis and ^{29}Si NMR

zeolite	chemical analysis	^{29}Si NMR
La(41)NaY	41	41
La(74)NaY	74	72
La(100)Y	100	100

in the curve fitting of LaNaY; both the functions **NaY** and **LaY** originate from this spectrum. When the experimentally derived spectra of LaNaY are curve-fitted by the two functions, only six values are varied, namely, chemical shift, line width, and amplitude for both. When a relatively good curve fitting was obtained, only small adjustments within the 10 peaks in LaNaY were necessary to obtain the best fit between the sum of **NaY** and **LaY** and the experimentally obtained spectra.

The results of this curve fitting are presented in Figure 5. The curve fittings of La(41)NaY and La(74)NaY give very high consistency between the curve-fitted and observed spectra. The relative ratios of the areas in **NaY** and **LaY** appear to give a direct representation of the Na/La composition as reported by Chao,¹¹ that is, the percent La exchange of the zeolite. The results derived from NMR and chemical analysis are compared in Table 2. In Figure 5b,d, the results of the full curve-fittings are presented, with all 10 peaks visible. The chemical shift, line width, and intensity of the 10 peaks in La(41)NaY are given in Table 3.

Zeolite X. In Figure 6 the spectra of as-exchanged samples of LaNaX and NaX are compared. A strong perturbation of the spectra of LaNaX is evident from the figure, as opposed to what was observed for hydrated zeolite Y (Figure 3). The line

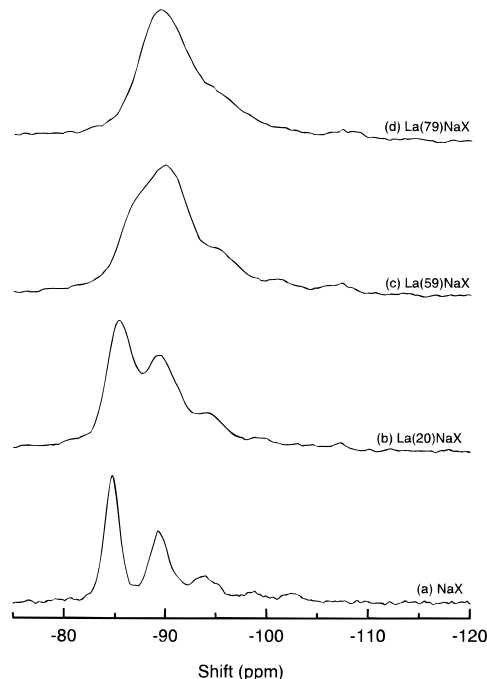


Figure 6. ^{29}Si MAS NMR spectra of as-exchanged samples of LaNaX and NaX: (a) NaX, (b) La(20)NaX, (c) La(59)NaX, and (d) La(79)NaX.

TABLE 3: ^{29}Si NMR Chemical Shift, Line Width, and Area of the Individual Peaks in La(41)NaY

Si(<i>n</i> Al)	chemical shift (ppm)		line width (ppm)		area	
	NaY	LaY	NaY	LaY	NaY	LaY
<i>n</i> = 4	-88.35	-90.76	4.02	4.02	0.19	0.12
<i>n</i> = 3	-92.37	-94.78	4.02	4.02	0.86	0.54
<i>n</i> = 2	-95.18	-98.39	2.81	3.61	1.74	1.28
<i>n</i> = 1	-99.20	-102.81	4.02	4.82	2.19	1.57
<i>n</i> = 0	-104.01	-107.23	5.62	6.02	0.69	0.45
				Si/Al	2.5	2.5

shapes are clearly different from NaX, and the increased line width with the level of lanthanum is obvious; while the peaks are well-separated in NaX and La(20)NaX, the individual lines in La(59)NaX and La(79)NaX are difficult to distinguish.

In Figure 7 the ^{29}Si NMR spectra of the calcined samples of LaNaX are presented. When the spectra of La(97)NaX and NaX are compared, the high-field shift of about 5 ppm as a result of lanthanum migration, and the increased line width for the lanthanum exchanged zeolites, can be clearly seen. The ion exchange of only 20% of the sodium cations with lanthanum results in a line shape very different from NaX. As more lanthanum is introduced, the line shape becomes more and more similar to La(97)NaX (and NaX), and the similarity between La(79)NaX and La(97)NaX is evident. For La(20)NaX, La(42)NaX, and La(59)NaX a shoulder at the same position as Si(4Al) in NaX can be seen, this being absent in La(79)NaX and La(97)NaX. The shoulder is strongest for La(20)NaX and is gradually diminishing as the level of lanthanum is increased.

In Figure 8 the spectra of NaX and La(97)NaX are decomposed into their five constituent peaks, assuming 100% Gaussian line shape for each. The Si/Al ratios calculated from the relative peak areas were found to be 1.3 for both NaX and La(97)NaX, indicating no significant change in the framework composition by dealumination. In the literature the low stability of the HX zeolites has been described.^{17,18} ^{29}Si NMR and XRD (not shown) of La(97)NaX confirm that there has not been any collapse of the structure during the ion-exchange and calcination procedure. (The zeolite is calcined twice, once in the ion-

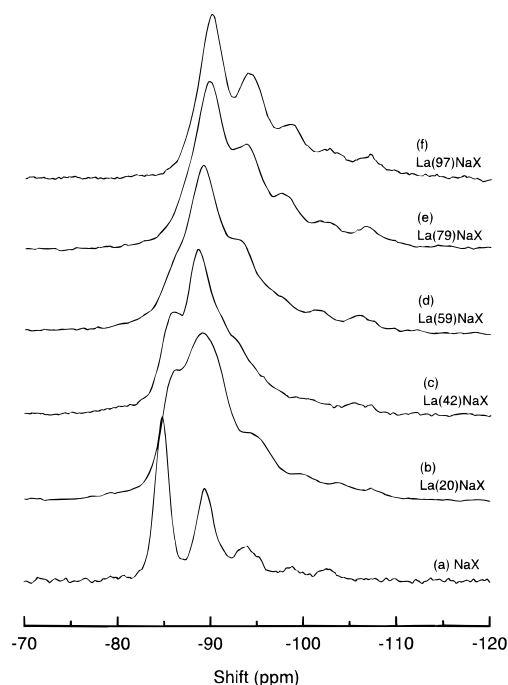


Figure 7. ^{29}Si MAS NMR spectra of calcined samples of LaNaX and NaX: (a) NaX, (b) La(20)NaX, (c) La(42)NaX, (d) La(59)NaX, (e) La(79)NaX, and (f) La(97)NaX.

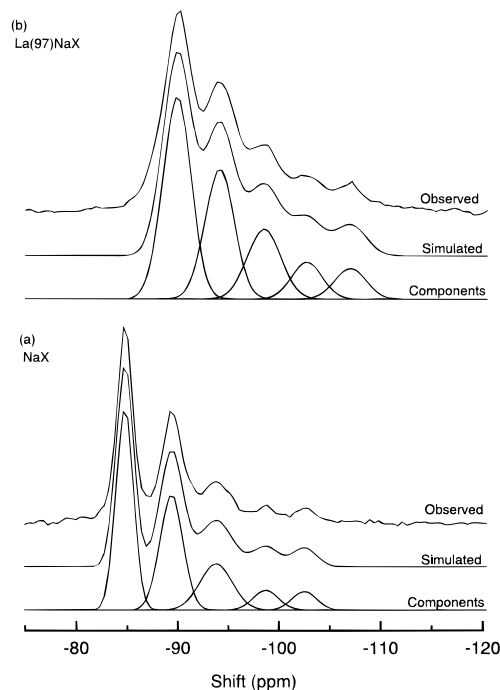


Figure 8. ^{29}Si MAS NMR spectra of (a) NaX and (b) La(97)NaX (calcined) decomposed into the constituent peaks.

exchange procedure and once prior to the NMR analysis.) This shows how lanthanum can contribute to the thermal stability of zeolite X.

Curve Fitting of LaNaX. Attempts to simulate the spectra of LaNaX in the same manner as was done for LaNaY were not successful. Thus, by using two functions **NaX** and **LaX**, derived from the spectrum of pure NaX, no reasonable representation of any of the LaNaX spectra could be obtained. This can apparently be attributed to a selective ion exchange of cations close to the Si(4Al) sites in zeolite X, resulting in a different area ratio between the Si(*n*Al) lines in **NaX** than in **LaX**. Alternative constraints were therefore applied in which a redistribution of intensity between the two functions was

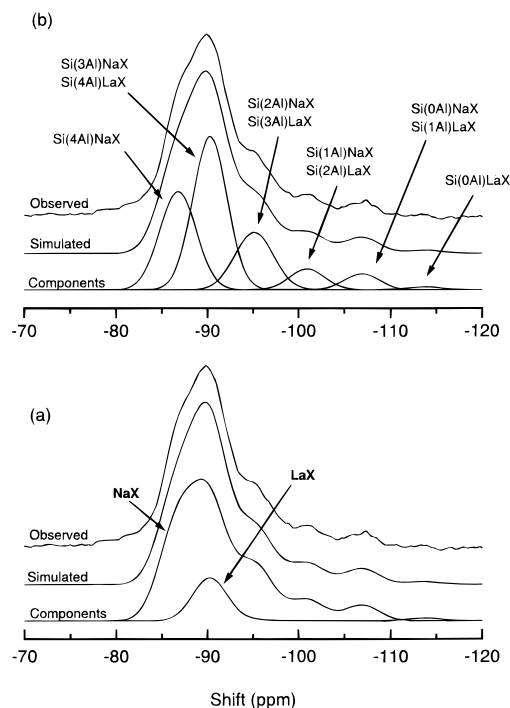


Figure 9. Observed and curve-fitted ^{29}Si MAS NMR spectrum of as-exchanged La(59)NaX including (a) the Na and La component profiles and (b) the full curve fitting, with all the constituent peaks visible.

allowed, while fixing the overall Si/Al ratio for the sum of the two functions, according to eq 1.

$$\text{Si/Al} = \frac{\sum (I_n^{\text{Na}} + I_n^{\text{La}})}{0.25 \sum n(I_n^{\text{Na}} + I_n^{\text{La}})} \quad (1)$$

where I_n^{Na} is the area of Si(*n*Al) in the **NaX** function and I_n^{La} the area of Si(*n*Al) in the **LaX** function.

The result of curve fitting of as-exchanged La(59)NaX according to (1) is presented in Figure 9a, and the high consistency between observed and simulated spectra is evident. The deconvolution of the spectrum into its constituent peaks is presented in Figure 9b. Even though the spectra of NaX and La(97)NaX both consist of five peaks (Figure 8), the spectrum of La(59)NaX was deconvoluted into only six different peaks. This can be explained by a total overlap of Si(3Al), Si(2Al), Si(1Al), and Si(0Al) in the unperturbed part of spectrum with Si(4Al), Si(3Al), Si(2Al), and Si(1Al) in the perturbed part, as indicated in the figure. Thus, the most low-field peak represents the Si(4Al) in **NaX** and the high-field peak the Si(0Al) in **LaX**.

Discussion

Curve Fitting. The results from the curve fitting of LaNaY presented in Figure 5 clearly show that the ^{29}Si spectra of the LaNaY zeolites can be separated into two sets of peaks, as reported by Chao et al.¹¹ However, Chao assumed the chemical shift and line width for the individual peaks to be constant, regardless of the lanthanum loading, and the Si/Al ratios, defined by each set of peaks, were kept equivalent to pure NaY. Hence, many variables were kept invariant. When the spectra of LaNaY were curve-fitted by the use of the Gaussian functions **NaY** and **LaY** in this work, the only assumption initially was the constant Si/Al ratio of the framework within each function. By regarding the spectra as a superimposition of two peaks, **NaY** and **LaY**, only six variables needed to be varied in the curve fitting to change the overall spectrum. It is evident from our results that the line widths and chemical shift of the individual peaks in LaNaY are not necessarily the same in a LaNaY with

a low lanthanum loading as in a fully exchanged zeolite, and the individual peaks do not necessarily vary with the same order of magnitude. A decrease in the separation in chemical shift for the peaks in La(100)Y is evident in Figure 4, where the peaks are closer than in NaY. Such small variations were automatically taken account of in our method.

Curve fitting of the different samples of LaNaX was more complicated than the curve fitting of LaNaY. This was apparently the result of a selective ion exchange of the cations close to the Si(4Al) sites in zeolite X. The results from the fit of all the as-exchanged samples of LaNaX clearly show that the Si(4Al) is selectively perturbed. Consequently, the relative ratio between the peak areas were altered, and the spectra can therefore not be simulated with the functions **NaX** and **LaX**, in which the relative peak areas are fixed. A selective decrease of the area of Si(4Al) in **NaX** is correlated with a equivalent increase of the area of Si(4Al) in **LaX**, and the overall Si/Al ratio will therefore remain constant when the area of the different Si(*n*Al) lines in the unperturbed and perturbed part of the spectra are added. The high consistency between the observed and simulated spectra of as-exchanged La(59)NaX, when it is curve-fitted according to eq 1, is a strong indication of such a selective ion exchange in zeolite X.

A selective ion exchange was also observed in a study of the ion exchange of the paramagnetic Cu²⁺ cation into NaX.¹⁹ The presence of small amounts of Cu²⁺ resulted in a selective disappearance of the Si(4Al) peak in the ²⁹Si NMR spectrum, due to the local effect of the paramagnetic copper.

Hydrated versus Calcined Samples. The spectrum of hydrated La(41)NaY presented in Figure 3 had a line shape and chemical shift similar to NaY, while the spectrum of the calcined sample showed different shape and peak position. This is also consistent with earlier results¹⁴ and is due to different locations of the lanthanum cations in hydrated and calcined samples. The ²⁹Si spectra are not perturbed by La cations in the supercage of zeolite Y, only by La cations in the sodalite cage.

In the LaNaX series, a quite different result was found. As can be seen in Figure 6, the spectra of the as-exchanged LaNaX are very different from the spectrum of the pure NaX. This difference must result from an interaction between the zeolite framework and either lanthanum cations in the sodalite cage (i) or lanthanum cations in the supercage (ii).

(i) If there are lanthanum cations in the sodalite cage, these must have migrated during the process of ion exchange. As described earlier, a dehydration of the lanthanum cation is necessary before this is possible. The dehydration requires energy, and for zeolite Y the migration is known to start at 80 °C. However, the lower energy needed to dehydrate the hydrated lanthanum cation in zeolite X compared to zeolite Y is reported.²⁰

(ii) It is evident from the curve fitting of the as-exchanged samples of LaNaX that there is a strong interaction between La³⁺ and the Si(4Al) sites, this species being absent in zeolite Y due to their high Si/Al ratio. It is thus possible that this interaction may be so strong that it can be observed by NMR, irrespective of the location of the cation in the supercage.

Compared with the results from zeolite Y, a perturbation of the ²⁹Si spectra by lanthanum cations in the supercage is difficult to understand. We therefore suggest (i) that the strong perturbation is caused by lanthanum cations in the sodalite cage. Further investigation is being undertaken to reveal the actual position of the lanthanum cation in the as-exchanged samples of LaNaX.

Correlation of NMR and Chemical Analysis (Zeolite Y). As described earlier, the ²⁹Si spectrum of a LaNaY zeolite is reported to reflect the level of lanthanum exchange, as demonstrated for La(41)NaY and up to La(100)Y. Considering that

the high-field shift of the lanthanum-exchanged zeolite is attributed to increased strain in a [SiO₄] tetrahedron in the vicinity of a lanthanum cation in the SI' site, the correlation between the level of lanthanum loading and the ²⁹Si spectrum should be expected to reflect the degree of occupancy of the SI' sites by lanthanum. In this work a zeolite with Si/Al = 2.5 was employed, and the maximum number of lanthanum cations that can be incorporated is therefore ca. 18.3. The unit cell in zeolite Y contains 32 SI' sites, and only a maximum of 56% of the ²⁹Si spectrum should therefore be influenced by lanthanum in the fully exchanged zeolite. However, the fraction of the spectra shifted upfield was consistent with the percentage of La exchange of Na rather than the percentage occupancy of the SI' site. It is also quite clear that 100% of the Si(*n*Al) lines were shifted ca. 3 ppm to higher magnetic field in the La(100)Y sample rather than 56% (Figure 4).

Evidently, our results and those of Chao do not agree with the theory above. Three possible explanations that can rationalize these apparent inconsistencies are as follows:

(i) One La³⁺ cation undergoes a rapid exchange between SI' sites within the NMR time scale.

(ii) Lanthanum occupies the SI site. The consistency between lanthanum loading and NMR could be rationalized if the lanthanum cations were located at SI, since zeolite Y only contains 16 SI sites per unit cell. Intuitively, one would expect SI in the hexagonal prism to be the preferred location, since a La³⁺ in a hexagonal prism would be octahedrally coordinated to six framework oxygen atoms while SI' enables coordination to only three. However, early structural studies⁵ and recent X-ray powder diffraction³ point to the SI' site as the favored site for the dehydrated cation, and this is also in accordance with the results from neutron diffraction.²¹ These results are also supported by computer modeling of lanthanum in the framework of faujasite, which indicates that La³⁺ cations located at SI' have the opportunity of achieving a coordination of six and that this position has a stability greater than that of the SI site.⁶

Thus, the current consensus of the literature is that the SI' site is the favored position of lanthanum in calcined LaNaY, and our spectra can therefore probably not be explained by (ii). A third possibility must also be included, even if it is unlikely that our observations can be rationalized by this.

(iii) When the lanthanum is exchanged with sodium cations in the sodalite cage, one lanthanum cation replaces three sodium cations. The net result is therefore two empty cation positions. The unfilled SI' sites in the region of Al may induce a perturbation of the ²⁹Si spectra that is equivalent to the presence of La³⁺.

As can be seen above, different theories may be given to explain our NMR spectra of LaNaY. In our opinion the most feasible explanation is the rapid motion of the cations, described in (i). Support for this conclusion may be found in a study of the introduction of paramagnetic Cu²⁺ into zeolite X.¹⁹ The perturbation of the ²⁹Si spectra was found to be more extensive than would be explained by the low amount of incorporated Cu²⁺; however, the effect was reduced when the NMR was recorded at a lower temperature. This result was attributed to reduced motion of the cations at lower temperature. A low-temperature study of the zeolites presented in our work could therefore probably either confirm or reject (i), and work in this direction is in progress.

Probing the Local Ordering of Framework Elements. Figure 10 presents an illustration of the contribution from (i) **LaX** and (ii) the Si(4Al) peak in **LaX** to the total area of the ²⁹Si NMR spectra of the as-exchanged samples of LaNaX. It is evident from Figure 10 that the area of **LaX** versus the

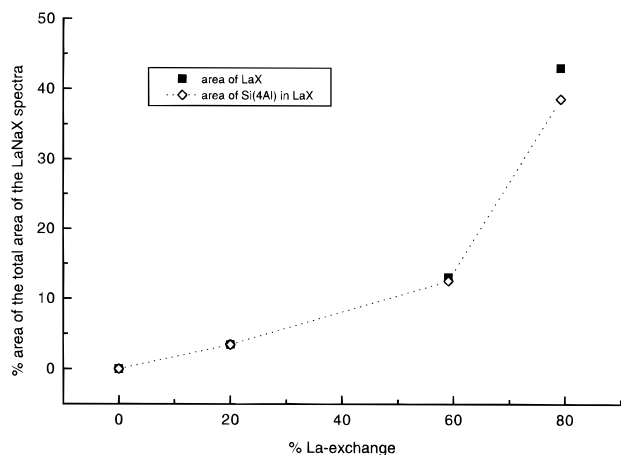


Figure 10. Contribution from (i) **LaX** and (ii) the Si(4Al) peak of **LaX** to the total area of the ^{29}Si NMR spectra of as-exchanged LaNaX, as a function of lanthanum exchange.

lanthanum content shows a nearly linear trend up to about 60% La exchange, and then a break in the curve can be seen. This indicates that something significant occurs after 60% ion exchange, which probably can be attributed to a selective introduction of lanthanum. The nearly overlapping symbols from the area of the Si(4Al) line in **LaX** and the total area of **LaX** indicate the disproportionate increase of the Si(4Al) line compared to the remaining lines and is a result of the selective lanthanum exchange.

As has been discussed already, the preferred location of the lanthanum cation is the SI' site. From the results of the curve fitting of LaNaX, it is evident that the La^{3+} cations were attracted to areas of high Al density. Accordingly, it will be expected that the SI' sites are more likely to be occupied by lanthanum when the aluminum content of the adjoining six-ring is high. The maximum number of aluminum atoms in a six-ring is three, since Al–O–Al linkages are excluded from the framework according to Löwenstein's rule.²² When lanthanum cations are introduced into the zeolite, one can therefore anticipate that the SI' sites connected to a six-ring containing three aluminum atoms will be occupied first. From a Monte Carlo simulation study of the distribution of Al in the faujasite structure,²³ it was found that in a zeolite with Si/Al = 1.3 about 53% of the six-rings containing three aluminums, with no differences observed in the cation distribution among double and single six-rings. This implies that 17 of the SI' sites per unit cell lie above six-rings containing three aluminum cations. Seventeen La^{3+} per unit cell correspond to an exchange level of 61% in this zeolite, in which all the La^{3+} cations should occupy SI' sites adjoining six-rings with three aluminums. From the break in the curve in Figure 10 it is evident that the function **LaX** contributes more to the total area of the spectra of LaNaX after about 60% ion exchange. Obviously, more of the ^{29}Si spectra will be affected by La when the lanthanum cations are close to several Si atoms, as is the case when the Al content of the nearby six-ring is low. The break in the curve at about 60% ion exchange can therefore probably be explained by occupation of SI' sites above six-rings with fewer than three aluminum cations at higher exchange levels. Hence, ^{29}Si NMR, in combination with selective exchange, may be used to study details of the local ordering of framework elements, as a complement to Monte Carlo simulations.

Conclusion

Curve fitting of lanthanum-exchanged zeolite Y with two functions **NaY** and **LaY** derived from the ^{29}Si NMR spectrum of pure NaY resulted in high consistency between the observed and simulated spectra when the Si/Al ratio of the framework within both functions were kept constant and similar to pure NaY. The fraction of the NMR spectrum affected by lanthanum was confirmed as being proportional to the total fraction of sodium replaced by lanthanum and not to the fractional occupancy of the SI' sites by lanthanum. Lanthanum-exchanged zeolite X could not be curve-fitted by two functions **NaX** and **LaX** derived from the spectrum of NaX with a fixed Si/Al ratio, due to a selective ion exchange of the cations close to the Si(4Al) sites in zeolite X. However, when a redistribution of intensity between the two functions was allowed, while keeping the overall Si/Al ratio fixed, high consistency between the observed and simulated spectra of LaNaX was found. It is evident from this work that lanthanum has a different impact on the framework in zeolite X than in zeolite Y. While hydrated samples of zeolite Y give similar ^{29}Si spectra to NaY, ^{29}Si spectra of as-exchanged LaNaX are strongly perturbed by lanthanum. The results from the combination of selective ion exchange and ^{29}Si NMR in zeolite X were found to correlate with Monte Carlo simulations and may be used as a complement in the study of the local ordering of framework elements. Further work will be undertaken to understand the different ^{29}Si NMR spectra from the two zeolites.

Acknowledgment. The authors are indebted to the Norwegian Research Council for their financial support of this work within the Strategic Technology Program. We also express our thanks to Aud Bouzga and Janett Simensen for technical assistance.

References and Notes

- (1) Biswas, J.; Maxwell, I. E. *Appl. Catal.* **1990**, *63*, 197.
- (2) Ikemoto, M.; Tsutsumi, K.; Takahashi, H. *Bull. Chem. Soc. Jpn.* **1972**, *45*, 1330.
- (3) Klein, H.; Fuess, H.; Hunger, M. *J. Chem. Soc., Faraday Trans.* **1995**, *91*, 1813.
- (4) Lee, E. F. T.; Rees, L. V. C. *Zeolites* **1987**, *7*, 143.
- (5) Bennett, J. M.; Smith, J. V.; Angell, C. L. *Mater. Res. Bull.* **1969**, *4*, 77.
- (6) Brennan, D.; Bell, R. G.; Catlow, C. R. A.; Jackson, R. A. *Zeolites* **1994**, *14*, 650.
- (7) Herreros, B.; Man, P. P.; Manoli, J.-M.; Fraissard, J. J. *Chem. Soc., Chem. Commun.* **1992**, 464.
- (8) Hunger, M.; Engelhardt, G.; Weitkamp, J. *Microporous Mater.* **1995**, *3*, 497.
- (9) Hunger, M.; Engelhardt, G.; Weitkamp, J. *Stud. Surf. Sci. Catal.* **1994**, *84*, 725.
- (10) Jelinek, R.; Malek, A.; Ozin, G. A. *J. Phys. Chem.* **1995**, *99*, 9236.
- (11) Chao, K.-J.; Chern, J.-Y.; Chen, S.-H.; Shy, D.-S. *J. Chem. Soc., Faraday Trans.* **1990**, *86*, 3167.
- (12) Gaare, K.; Akporiaye, D. *J. Mol. Catal.* **1996**, *109*, 177.
- (13) Carvajal, R.; Chu, P.-J.; Lunsford, J. H. *J. Catal.* **1990**, *125*, 123.
- (14) Chao, K.-J.; Chern, J.-Y. *J. Phys. Chem.* **1989**, *93*, 1401.
- (15) Venuto, P. B.; Hamilton, L. A.; Landis, P. S. *J. Catal.* **1966**, *5*, 484.
- (16) Fyfe, C. A.; Thomas, J. M.; Klinowski, J.; Gobbi, G. C. *Angew. Chem., Int. Ed. Engl.* **1983**, *22*, 259.
- (17) Otouma, H.; Arai, Y.; Ukihashi, H. *Bull. Chem. Soc. Jpn.* **1969**, *42*, 2449.
- (18) Ward, J. W. *Zeolite Chemistry and Catalysis*; American Chemical Society: Washington, DC, 1976; Chapter 3.
- (19) Kwak, J. H.; Ryoo, R. *J. Phys. Chem.* **1993**, *97*, 11154.
- (20) Sherry, H. S. *J. Colloid Interface Sci.* **1968**, *28*, 288.
- (21) Cheetham, A. K.; Eddy, M. M.; Thomas, J. M. *J. Chem. Soc., Chem. Commun.* **1984**, 1337.
- (22) Loewenstein, W. *Am. Mineral* **1954**, *39*, 92.
- (23) Herrero, C. P. *J. Phys. Chem.* **1991**, *95*, 3282.